Optics Letters

Liquid-crystal-based fiber laser sensor for non-invasive gas detection

Dong Zhou,[1] Qingxiu Wang,[1] Zeqing Lan,[1] Yuzhou Chen,[1] Zenghui Peng,[2] Lingli Zhang,[3,4] and Yongjun Liu[1,2,*]

[1]Key Lab of In-fiber Integrated Optics, Ministry Education of China, Harbin Engineering University, Harbin 150001, China
[2]State Key Laboratory of Applied Optics, Changchun Institute of Optics, Fine Mechanics and Physics, Chinese Academy of Sciences, Changchun 130033, China
[3]School of Physics, Harbin Institute of Technology, Harbin 150001, China
[4]zhanglingli@hit.edu.cn
*liuyj@hrbeu.edu.cn

Received 16 March 2023; revised 19 July 2023; accepted 3 August 2023; posted 3 August 2023; published 21 August 2023

This Letter reports a new optical fiber gas sensor for measuring breath acetone. The sensor is based on photonic bandgap (PBG) mode laser emission sensing technology using liquid crystal (LC), which is combined with silica fiber and chiral nematic liquid crystal (CNLC), thus providing an ultra-compact, fast-response and simple-to-produce sensing system with a fast response that can accurately and quantitatively determine the concentration of respiratory acetone within the normal oral temperature range (35–38°C). Since LCs are affected by temperature, we propose a method that eliminates the influence of the temperature to solve the problem of the temperature influence when measuring gas. The detection of acetone leads to splitting of the dual laser peaks, with a linear correlation of 0.99. The sensor has a limit of detection of 65 ppm for acetone vapor and thus is suitable for breath acetone detection in diabetic patients.

https://doi.org/10.1364/OL.489552

Variations in human respiratory acetone levels are associated with ketosis, which is the production of ketone bodies from the oxidation of non-esterified fatty acids [1]. Ketone bodies are by-products of fat metabolism that include β-hydroxybutyrate and acetone. These two ketone bodies end up undergoing enzymatic degradation or spontaneous decarboxylation. The increase in acetone may be caused by diabetic ketoacidosis and a high-fat diet, and acetone is a reliable indicator of ketone body circulation [2]. An increase in acetone levels is accompanied by the possibility of diabetes. However, biomedical measurement regarding diabetes in humans currently relies on blood glucose analysis. Acetone levels can rise to 40 ppm in adults on a ketogenic diet [3] and to 360 ppm in children with epilepsy who rely on high-fat and low-carbohydrate diets [4]. Poorly controlled diabetes can lead to ketoacidosis, in which acetone can increase to 1250 ppm [5]. In fact, the correlation between blood glucose and breath acetone has been validated, and breath acetone analysis can be used to identify and monitor clinical diagnostic procedures [6].

In recent years, the increasing emergence of non-invasive screening techniques has gradually compensated for the shortcomings of traditional diagnostics, and they now serve an important role in the diagnosis, prevention, treatment, and evaluation of diseases, such as in the diagnosis of respiratory acetone utilizing LAPS (light-addressable potentiometric sensors) [7], in the detection of the concentration of acetone in exhaled breath using a mass spectrometer [8], and in the measurement of acetone vapor by a MEMS (microelectromechanical systems)-based sensor for the non-invasive screening of diabetes [9]. Although these methods have certain advantages in gas detection, they also have deficiencies, such as the need for expensive and bulky equipment and complicated experimental preparation. In the future, non-invasive diagnosis will replace traditional diagnosis methods in medical clinical diagnosis and screening.

Liquid crystal (LC) materials with high birefringence have been comprehensively used in sensing fields such as biological [10], electric field [11], and pH [12] detection. At the same time, LCs are used for the measurement of chemical gases. For example, Li *et al.* developed a polymer cholesteric liquid crystal film to detect acetone vapor [13], Sutarlie *et al.* developed an LC polymer array to detect gaseous amines [14], Li *et al.* developed a blue-phase liquid crystal fiber-based device for sensing organic vapor [15], Batir *et al.* used a polydimethylsiloxane (PDMS)-based photonic interpenetrating network LC film to detect gas [16], and Bolleddu *et al.* transformed the phase transition of organic vapor to LC droplets into electrical signals for use in sensors [17]. However, there are some issues with these techniques, including the influence of temperature, the limitation of semi-quantitative detection, and the high limit of detection (LOD). Therefore, we proposed optical fiber as a carrier for LC and quantitatively detected the gas concentration using its liquid crystal spectrum. In our previous work [18], liquid-crystal-based optical fiber gas sensing was both affected by temperature and had a broad reflection spectrum with a high detection limit, so a new detection method is urgently needed to solve these problems.

In chiral nematic liquid crystal (CNLC), the director spontaneously twists along the direction perpendicular to the long axis of the molecule due to the chiral molecules. The periodicity generated by this helical twisting leads to a one-dimensional photonic bandgap structure, i.e., when circularly polarized light

propagates along the helix axis, the CNLC can reflect circularly polarized light with the same handedness as the helix direction. When optically pumped with a pulsed laser, the photonic band edges of dye-doped CNLC (DDCNLC) can achieve low-threshold mirrorless lasing [19]. The wavelength of the laser emission corresponds to the reflection band edge of the CNLC, which can be tuned by shifting the reflection band within the fluorescence emission spectral range of the laser dye [20].

Herein, for the first time, we develop a temperature-effect-eliminating gas sensor based on photonic bandgap (PBG) mode lasing for the detection of breath acetone using a 2×2 multimode fiber splitter. This sensor is a fiber probe with hollow capillary fibers (HCFs) that are filled with polyglycerin-10 and DDCNLC. When the pulsed laser is coupled to the fiber, the emission spectrum of the sensor exhibits a sharp single peak in the PBG mode. The proposed sensor is applied to the measurement of breath acetone for the first time and solves the problem that the sensor is affected by temperature in the human oral temperature range. Ultimately, the sensor will realize the real-time detection of human breath acetone.

Chiral dopants (R811, 25 wt. %) were added to form CNLC after nematic liquid crystal E7 (from Chengzhi Yonghua, 74 wt. %) had been sonicated for 20 mins. R811 was purchased from Beijing Inno-Chem. The laser dye 4-dicyano-methylene-2-methyl-6-(4-dimethylaminostyryl)-4H-pyan (DCM, from Exciton) with a concentration of 1 wt. % was added to CNLC as the gain medium. Polyglycerin-10 (from Yousuo Chemical) was used as an alignment agent in the experiment. UV curing glue (LEAFTOP 9310, from Shenzhen Tegu) was used as the sealing material for the fiber. A gas chamber with a capacity of 100 ml was used in the experiments. The fabrication process of the optical fiber sensing probe is shown in Fig. S1 in Supplement 1. When DDCNLC was filled into glycerol-containing HCF-100, the DDCNLC self-assembled into radial structures within 10 mins [21]. Polarized optical microscopy images of the liquid crystal after self-assembly are shown in Fig. S2 in Supplement 1 .

Figure 1 shows the configuration of the experimental system. The pumping source used a frequency-doubled Nd:YAG pulsed laser ($\lambda = 532$ nm, pulse duration 8 ns, repetition rate 5 Hz). The pump laser was passed through the objective (40×) and coupled into a 2×2 optical fiber splitter (port 1). The output ends of the optical fiber splitter were connected to the temperature probe (port 2) and the gas probe (port 3) located in the water bath temperature control system (temperature control accuracy ≤0.5°C), respectively. The spectral signals from the excited DDCNLC were collected via port 4 and transmitted to a high-speed optical spectrum analyzer (OSA; PG2000; the spectral resolution was 0.04 nm and the spectral range was 550–650 nm).

The lasing peak appears on the edge of either λ_1 or λ_2, depending on the appropriate relative positions of the LC reflection and

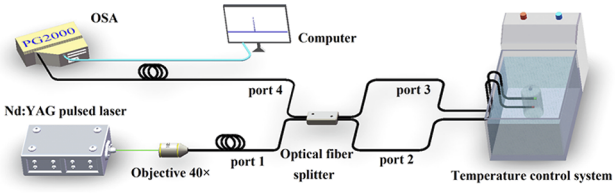

Fig. 1. Schematic diagram of the optical fiber gas sensing experimental system based on DDCNLC.

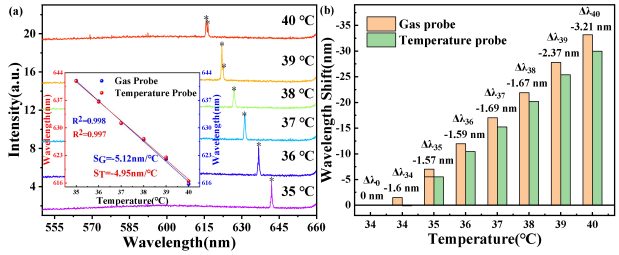

Fig. 2. (a) Dual-lasing spectrogram influenced only by the temperature in the absence of gas. Inset: dual-lasing wavelength as a function of temperature. (b) Relationship between the dual-lasing wavelength difference ($\Delta\lambda$) for quantitatively detecting acetone in the gas chamber and the temperature.

fluorescence peaks. The positions of the edges of the reflection band wavelengths are $\lambda_1 = n_e p$ and $\lambda_2 = n_o p$, respectively. $p = 1/(\beta c)$ is the helical pitch, c is the concentration of the chiral dopant, and β is the helical twisting power [22]. In other words, the lasing peak depends on where the dye gets the optimal gain [23]. When the reflection band edge is close to the fluorescence emission wavelength of the DCM dye, the reflection band edge can be amplified, generating the PBG.

All LCs are sensitive to temperature, which seriously affects the gas measurement results. Therefore, we propose a method that eliminates the influence of the temperature. A temperature probe and a gas probe containing the same LC produce the same PBG laser peak. If the temperature changes when the gas is detected, the wavelength difference ($\Delta\lambda = \lambda_{gas} - \lambda_{temperature}$) between the two laser peaks will be unchanged with temperature, resulting in the elimination of the influence of the temperature on the sensor. Figure 2(a) is the laser spectrum when it is only affected by the temperature. The inset exhibits the dependence of $\Delta\lambda$ on the temperature in the absence of any gas. The results showed that the $\Delta\lambda$ between the two PBG laser peaks did not change in the normal oral temperature range (35–38°C). In order to further validate the minimal influence of the temperature on the $\Delta\lambda$ between the two PBG laser peaks, we maintained a constant concentration of acetone in the gas chamber. We then observed whether the $\Delta\lambda$ between the two laser peaks was affected as the temperature increased. When the two fiber probes were placed in a toxic gas chamber containing a small amount of acetone, the gas probe's laser wavelength underwent a shift. At this point, the acetone concentration was kept constant, and the sensor was only influenced by the temperature, as shown in Fig. 2(b). The $\Delta\lambda$ between the two peaks was 0 nm at 34°C. But, as the acetone concentration was increased, the gas probe was affected by the gas, and the laser peak split into two PBG laser peaks. The detection of acetone was influenced by temperature fluctuations, resulting in a slight wavelength shift. There was almost no change in the $\Delta\lambda$ between the two peaks with increasing temperature, but the $\Delta\lambda$ increased slightly when the temperature rose to 39°C. In conclusion, Fig. 2 shows a slight increase in $\Delta\lambda$ as the temperature rises to 39°C, which may be due to the influence of the cavity air pressure in the sealed temperature probe. Therefore, this could lay the foundations for the detection of breath acetone in the human oral cavity.

Because the temperature sensitivity of the two optical fiber probes is the same, the wavelength difference between the PBG lasers generated by the two probes when sensing the gas is only

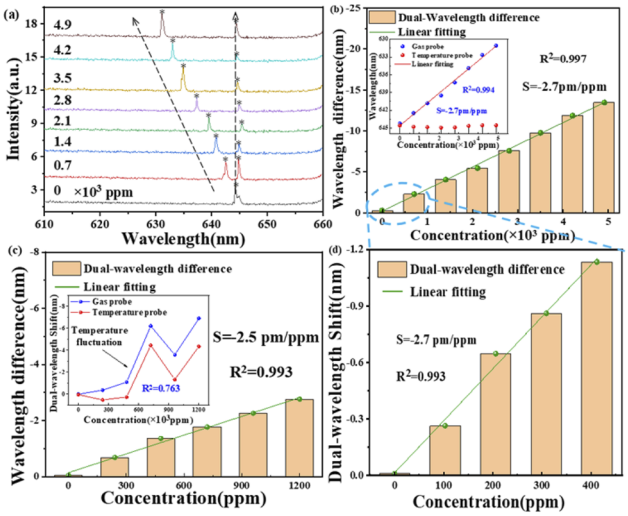

Fig. 3. (a) Change in the dual-lasing emission spectrogram with increasing acetone concentration for slight temperature fluctuations. (b) Change in the dual-lasing $\Delta\lambda$ with increasing acetone concentration. Inset: real-time detection of acetone concentration and the dual-lasing peak wavelength dependence. (c) Relationship between dual-lasing $\Delta\lambda$ and acetone concentration when influenced by temperature fluctuations. Inset: Dual-lasing wavelength change relationship subject to temperature fluctuations when measuring acetone. (d) Dependence of the dual-lasing $\Delta\lambda$ on the concentration of acetone at acetone concentrations.

affected by the gas concentration. Figure 3(a) shows the laser spectrum obtained when measuring acetone vapor. The sensor was placed in the gas chamber and 0.2 μL of acetone were titrated at a time. Since the temperature probe was sealed with UV-curing glue, the laser peak it produced was only affected by temperature. When acetone was not titrated, the laser peaks of the two probes were almost completely superimposed. But, as the acetone concentration increased, the gas probe was affected by the gas, and the laser peak split into two PBG laser peaks. The detection of acetone was influenced by temperature fluctuations, resulting in a slight wavelength shift. The key factors that cause the blueshift of λ are an inclination of the helical axis of the LC, a reduction in the elastic constant, a decrease in the refractive index, and π-π stacking [24]. Different chiral agents also have different sensitivities to the acetone response (see Table S1 and Fig. S3 in Supplement 1), and this sensitivity may be determined by the rigid group. Compared with the other three chiral agents, R811 has fewer rigid groups and a higher sensitivity to the acetone response. Figure 3(b) shows the resonance $\Delta\lambda$ generated by the two probes after temperature elimination, which further verifies that there is a good linear relationship between the gas concentration and the $\Delta\lambda$. The inset shows the sensitivity and linearity of the sensor with respect to acetone concentration in the absence of temperature elimination. Slight fluctuations in temperature cause a slight decrease in the linearity of this sensor for gas sensing.

To obtain a low LOD, we titrated the minimum dose of acetone, and the results are shown in Fig. 3(d). This result is as expected, with the same linear correlation and sensitivity as in Fig. 3(b). Figure 3(c) shows that the dual-lasing $\Delta\lambda$ can be considered as a temperature-independent acetone measurement with a linear fit of 0.99. The sensitivity deviation comes from

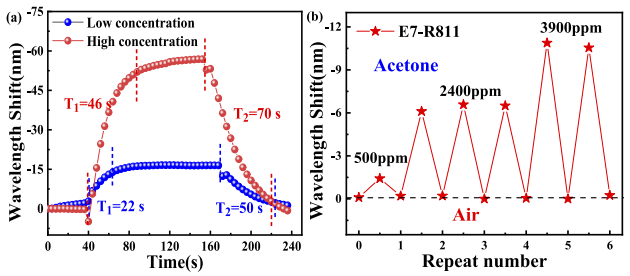

Fig. 4. (a) Sensor response time to acetone. (b) Repeatability of the sensor in gas chambers with different acetone concentrations.

minor variations in the amount of acetone solvent injected into the gas chamber each time and the accumulated deviations in the selection of data points. As shown in the inset of Fig. 3(c), when the acetone concentration was measured, the temperature fluctuated. The temperature fluctuation between 35.5 and 37°C leads to a linear correlation coefficient of 0.763, which means that there is not a linear correlation in this case. Meanwhile, for the linear calibration curve, the LOD in a limited concentration range can be expressed as LOD = $3S_a/b$ [25], where S_a is the standard deviation of the response and b is the slope of the calibration curve. The theoretical calculation of the LOD value is 65 ppm.

The laser wavelength response time and repeatability are important parameters when testing gas-sensitive properties. Figure 4(a) presents the sensor's response time to acetone detection. Whether it was a low concentration or high concentration of acetone, the response time of the sensor was within 50 s. The response time decreased with decreasing acetone concentration, but the recovery time was generally twice the response time. The slight wavelength shift of the blue dots within the 0–40 s interval is attributed to the presence of a small amount of residual acetone gas in the gas chamber. Figure 4(b) shows the repeatability of the gas sensor. To obtain repeatability data for this sensor at different concentrations, three acetone concentrations were used to test the performance of the sensor. After complete evaporation of the acetone, we sequentially placed the sensor in gas chambers containing different concentrations of acetone. During all cycles, the wavelength returned to its initial position when the sensor was placed in the air. In order to ensure that the sensor in the gas chamber was in full contact with acetone and the sensor was exposed to air without any residual gas, the switching time of the sensor in the gas chamber and in the air was 5 mins. As expected, the detection of the sensor is reversible.

Patients with diabetes have lower levels of insulin, which is used to inhibit ketone synthesis, and have higher levels of exhaled acetone [26]. The presence of comorbidities further complicates exhaled breath analysis; for example, people with both stage C heart failure and diabetes exhale higher amounts of acetone [27]. Different combinations of the three exhaled gas components (i.e., acetone, ethanol, and propanol) all correlate with estimated blood glucose values [28]. To validate the PBG-laser-sensor-based detection of respiratory acetone, seven adult volunteers participated in a study. None of the subjects smoked, took long-term medications, or had known chronic diseases. The first six volunteers all collected their exhaled breaths before lunch, and the last volunteer collected the gas at different points in time. When measuring each exhaled breath, it was injected

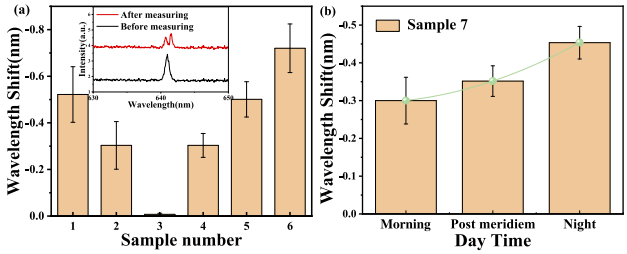

Fig. 5. (a) Relationship between wavelength and acetone exhaled before lunch in six adult volunteers. Inset: dual-lasing spectrogram for the measurement of the sixth gas sample. (b) Breath acetone as a function of wavelength at different points in the day from one adult volunteer.

into a vacuum gas sample bag (100 mL) to exclude the influence of other gas molecules.

The detection results for the exhaled breaths of different volunteers are presented in Fig. 5. Figure 5(a) shows the measurement results for six gas samples, and the inset shows the spectrum of detection sample 6. Both samples 1 and 5 belonged to patients who had suffered mild diabetes for 5 years, while samples 2 and 4 belonged to patients who had suffered mild diabetes for 4 and 7 years, respectively. Sample 3 was from a patient with newly detected mild diabetes, while sample 6 was from a patient with severe diabetes. The analysis revealed that sample 6 had a gas content that was noticeably higher than those in the other samples. Figure 5(b) shows the detection results for exhaled breaths from the same severe diabetic patient at different time points. During the morning fasting state, acetone is produced from lipolysis and lipid oxidation as an energy substrate [2], so the acetone concentration in exhaled breath is lower. But, after lunch and evening meals, acetone levels tended to rise.

Traditional diabetes detection is mainly based on blood glucose analysis. This paper has proposed a non-invasive method for disease detection. Meanwhile, a new liquid-crystal-based light gas sensor was developed that can be used to measure human breath acetone. The proposed sensor has the characteristics of a fast response, simple production, and the quantitative detection of the acetone concentration by a PBG mode laser with high recognition. We have proposed a method that eliminates the influence of the temperature and utilizes dual-laser wavelength difference ($\Delta\lambda$) sensing of the acetone concentration. The effect of temperature fluctuations can be eliminated even when acetone is detected. The sensor can accurately detect acetone and is not affected by the temperature within the range of body temperature. The performance of the sensor was further verified by collecting and detecting respiratory acetone from different diabetic patients.

Funding. National Natural Science Foundation of China (Grant No. U1531102), Fundamental Research Funds for the Central Universities

Disclosures. The authors declare no conflicts of interest.

Data availability. Data underlying the results presented in this paper are not publicly available at this time but may be obtained from the authors upon reasonable request.

Supplemental document. See Supplement 1 for supporting content.

REFERENCES

1. K. Musa-Veloso, E. Rarama, F. Comeau, R. Curtis, and S. Cunnane, Pediatr. Res. **52**, 443 (2002).
2. O.E. Owen, S. Caprio, G.A. Reichard Jr., M.A. Mozzoli, G. Boden, and R.S. Owen, Clin. Endocrinol. Metab. **12**, 359 (1983).
3. L. R. Saslow, S. Kim, J. J. Daubenmier, J. T. Moskowitz, S. D. Phinney, V. Goldman, E. J. Murphy, R. M. Cox, P. Moran, and F. M. Hecht, PLoS One **9**, e91027 (2014).
4. K. Musa-Veloso, S. S. Likhodii, E. Rarama, S. Benoit, Y.-M. C. Liu, D. Chartrand, R. Curtis, L. Carmant, A. Lortie, F. J. E. Comeau, and S. C. Cunnane, Nutrition **22**, 1 (2006).
5. A. E. Jones and R. L. Summers, J. Emerg. Medicine **19**, 165 (2000).
6. M. Boubin and S. Shrestha, Sensors **19**, 2283 (2019).
7. Q. Zhang, P. Wang, J. Li, and X. Gao, Biosens. Bioelectron. **15**, 249 (2000).
8. J. C. Anderson, W. J. E. Lamm, and M. P. Hlastala, J. Appl. Physiol. **100**, 880 (2006).
9. A. A. S. Rabih, J. O. Dennis, A. Y. Ahmed, M. H. M. Khir, M. G. A. Ahmed, A. Idris, and M. U. Mian, IEEE Sens. J. **18**, 9486 (2018).
10. C. L. Xia, D. Zhou, Y. M. Su, G. K. Zhou, L. S. Yao, W. M. Sun, and Y. J. Liu, Analyst **145**, 4569 (2020).
11. M. Humar, Liq. Cryst. **43**, 1937 (2016).
12. Y. Wang, L. Y. Zhao, A. J. Xu, L. Wang, L. L. Zhang, S. Q. Liu, Y. J. Liu, and H. Y. Li, Sens. Actuators, B **258**, 1090 (2018).
13. Y. Li, Z. Yin, and D. Luo, Opt. Express **30**, 32822 (2022).
14. L. Sutarlie, H. Qin, and K. L. Yang, Analyst **135**, 1691 (2010).
15. Y. Li, Z. Yin, and D. Luo, Opt. Lett. **48**, 89 (2023).
16. O. Batir, E. Bat, and E. Bukusoglu, Sens. Actuators, B **367**, 132172 (2022).
17. R. Bolleddu, S. Chakraborty, M. Bhattacharjee, N. Bhandaru, S. Thakur, P. S. Gooh-Pattader, R. Mukherjee, and D. Bandyopadhyay, Ind. Eng. Chem. Res. **59**, 1902 (2020).
18. Y. H. Yang, D. Zhou, X. J. Liu, Y. J. Liu, S. Q. Liu, P. X. Miao, Y. C. Shi, and W. M. Sun, Opt. Express **28**, 31872 (2020).
19. M. Humar and I. Musevic, Opt. Express **18**, 26995 (2010).
20. S. M. Wood, F. Castles, S. J. Elston, and S. M. Morris, RSC Adv. **6**, 31919 (2016).
21. F. Xu and P. P. Crooker, Phys. Rev. E **56**, 6853 (1997).
22. D. Zhou, Z. Q. Lan, W. Z. Cao, Y. Z. Chen, S. S. Zhang, J. Y. Hu, J. Y. Shang, Z. H. Peng, and Y. J. Liu, Opt. Laser Technol. **156**, 108545 (2022).
23. J. Liu, Y. J. Chen, F. Jin, J. X. Wang, T. Ikeda, and L. Jiang, Adv. Mater. **34**, 2108330 (2022).
24. K. J. Kek, J. J. Z. Lee, Y. Otono, and S. Ishihara, J. Soc. Inf. Disp. **25**, 366 (2017).
25. A. Shrivastava and V. Gupta, Chron. Young Sci. **2**, 21 (2011).
26. C. Turner, C. Walton, S. Hoashi, and M. Evans, J. Breath Res. **3**, 046004 (2009).
27. T. Yokokawa, T. Sato, S. Suzuki, M. Oikawa, A. Yoshihisa, A. Kobayashi, T. Yamaki, H. Kunii, K. Nakazato, H. Suzuki, S. Saitoh, T. Ishida, A. Shimouchi, and Y. Takeishi, BMC Cardiovasc. Disord. **17**, 280 (2017).
28. S. Mansouri, S. Boulares, and T. Alhadidi, IEEJ Trans. Electr. Electron. Eng. **15**, 1457 (2020).